Hydrogen Ion Block of the Sodium Pore in Squid Giant Axons

TED BEGENISICH and MIKLOS DANKO

From the Department of Physiology, University of Rochester School of Medicine, Rochester, New York 14642

ABSTRACT   The block of squid axon sodium channels by H ions was studied using voltage-clamp and internal perfusion techniques. An increase in the concentration of internal permeant ions decreased the block produced by external H ions. The voltage dependence of the block was found to be nonmonotonic: it was reduced by both large positive and large negative potentials. The ability of internal ions to modify the block by external H^+ is explained by a competition among these ions for a binding site within the pore. The nonmonotonic voltage dependence is consistent with this picture if the hydrogen ions are allowed to be permeant.

INTRODUCTION

External hydrogen ions can inhibit sodium channel currents in many nerve and muscle preparations (Hille, 1968; Drouin and The, 1969; Shrager, 1974; Schauf and Davis, 1976; Campbell and Hille, 1976). Woodhull (1973) showed that the inhibition depends upon membrane voltage, and from this she concluded that hydrogen ions bind to a site within the sodium pore. Drouin and Neumcke (1974) proposed an alternative mechanism whereby hydrogen ions reduce the permeant ion concentration near the entrance to the pore by titrating a local surface charge. In this view the hydrogen ion site is external to the pore and the voltage dependence arises from a change in the rectification of the current-voltage relation of the pore.

In this paper we have attempted to resolve the issue of whether or not the hydrogen ion binding site is within the pore. We find that internal permeant ions reduce the effectiveness of external hydrogen ions, which we take as a demonstration that the binding site is within the sodium channel permeation pathway. We also investigated the voltage dependence of H^+ block using instantaneous current-voltage relations. We find that the block is a non-monotonic function of voltage: hydrogen ions are less effective at both large negative and large positive membrane potentials. These results can be quantitatively accounted for by a three-barrier, two-site model for ion permeation

(Begenisich and Cahalan, 1980a, b). In terms of the model, the decrease in block at positive potentials occurs because these potentials reduce the binding of hydrogen ions within the pore. The relief of block at negative potentials results from the hydrogen ions being driven through the pore. A preliminary report of this work has been given (Begenisich and Danko, 1982).

METHODS

The methods used in this study have been described before (Begenisich and Lynch, 1974; Busath and Begenisich, 1982). Live squid, Loligo pealei, were obtained from the Arrive Alive Biological Supply Company, Greenport, NY. The method of capture, transportation, and maintenance of the animals has been recently described in detail.[1]

The diameter of the 20 axons used in this study ranged from 375 to 675 μm, with an average of 475 μm. All potentials were corrected for liquid junction potentials. The resting potential of axons bathed in normal artificial seawater and internally

TABLE I
Composition of Internal and External Solutions

	External					
	Na	Ca	Mg	Glycine	Hepes	Citrate
	mM			mM		mM
ASW	440	10	50	0	10	0
0 Mg ASW	440	10	0	200	10	20

	Internal						
	Na	K	Cs	F	Glutamate	Glycine	Phosphate
	mM						
50 Na SIS	50	0	150	150	—	685	25
200 Na SIS	200	0	0	100	50	700	25
25 Na SIS	25	225	100	100	220	400	15
125 Na SIS	125	225	0	100	220	400	15
K SIS	0	350	0	50	270	390	15

perfused with K SIS (see below) averaged −65.7 mV. A temperature of 10°C was used in all experiments.

Normal artificial seawater (ASW) usually contains 10 mM Ca and 50 mM Mg (Table I). These ions block sodium channels in a voltage-dependent manner (Woodhull, 1973; Taylor et al., 1976; Busath and Begenisich, 1982) and could obscure the hydrogen ion effects. We therefore used the 0-Mg ASW containing 10 mM Ca shown in Table I. Early experiments showed no difference between 5 and 10 mM Ca, so the larger value was used because the axons survived better in this solution. The actual concentration of calcium was probably lower than 10 mM because of complexation with citrate. The other solutions used in this study are listed in Table I. The 0-Mg ASW solution contained 20 mM citrate ($pK_1 = 3.14$, $pK_2 = 4.77$, $pK_3 = 6.39$)

[1] Caufield, E., T. Caufield, R. S. Morello, L. Chabala, D. Busath, M. Danko, C. Smith, and T. Begenisich. Capture, transportation, and maintenance of live squid (Loligo pealei) for electrophysiological studies. Manuscript in preparation.

and 10 mM Hepes (pK_a = 7.55) as buffers. The internal solutions were buffered (to pH 7.5) with 15–25 mM phosphate.

Data acquisition and analysis techniques have been previously described (Begenisich and Busath, 1981). Briefly, an analog-digital converter operating under computer control sampled sodium channel current usually at 10- or 20-μs intervals. In most experiments tetrodotoxin (TTX) was added to the external solution and all pulse-protocol and solution changes were repeated. This provided a means to subtract non-sodium channel current from records of total current.

Electronic compensation for series resistance values of 3.2–6.3 Ωcm² (average of 4.6 Ωcm²) were used. Busath and Begenisich (1982) describe improvements made in the series resistance compensation of the voltage-clamp electronics. Briefly, these changes provide more complete compensation and a faster capacitative transient (complete within 10 μs, often within 8 μs; see Busath and Begenisich [1982] for a typical record). Integration of the capacitative transient shows that the membrane potential change is 90% complete within <5 μs. These improvements are especially important for measurement of sodium channel "tail" currents, which are both large and fast.

Changes in the hydrogen ion concentration bathing a nerve can alter the membrane surface potential, resulting in a modification of sodium channel gating properties (Hille, 1968; Carbone et al., 1978; and see Fig. 6). In these experiments we used "instantaneous" currents as a measure of the current through sodium pores.

A sample experiment illustrating how instantaneous currents were obtained is shown in Fig. 1. The inset shows sodium channel currents after TTX correction. A conditioning pulse to +10 mV was used to activate most (if not all) of the sodium channels. The length of the conditioning pulse (800 μs in this case) was chosen so that the current declined to approximately half of the peak value. This was done to allow sufficient time for all available channels to open. If this is not done, nonmonotonic "tail" currents at large positive test potentials may result as new channels open. The instantaneous current values for the test potential were obtained by fitting a single exponential to the early part of the tails and extrapolating back to the time of the change in potential.

Plotted semilogarithmically in the figure are the values of current recorded after the change in membrane potential to −60, −70, −80, and −90 mV. The current values are plotted (filled circles) at 10-μs intervals starting at 30 μs. A single exponential was fit to the first seven points (30–100 μs) of each record and extrapolated back to the time of the change in potential. The semilogarithmic plot illustrates that the time courses of the sodium channel tail currents are not single-exponential functions of time. However, for the first 100 μs a single exponential is a good approximation.

The purpose of this fitting procedure is not to develop a description of sodium channel gating kinetics. Rather, it is a means of obtaining the zero time value of current after a change in membrane potential. The procedure is valid if the membrane potential change is fast and if no alterations in sodium channel gating occur within the first 30 μs. The first condition is met since the fastest tail time constants are ∼50 μs, 10 times slower than the settling time of the membrane potential. In the absence of any evidence against the second assumption, we feel that the procedure described here is a reasonable method of obtaining data on the permeation properties of sodium pores independent of channel gating.

For the axon of Fig. 1 the zero time (instantaneous) currents were obtained both with and without a preconditioning hyperpolarizing prepulse. These currents are plotted in Fig. 2 as a function of the test potential. The values of the instantaneous

current without a preconditioning hyperpolarizing prepulse have been scaled by 1.68. The similarity of the shape of these two curves in the face of such a large difference in absolute current magnitudes argues for little, if any, contribution from uncompensated series resistance.

In most experiments, measurements of current were done both before and after exposure to a pH 4.8 solution. In these cases we averaged the control and recovery currents and computed the ratio of current in low pH to the average value at normal pH (7.5).
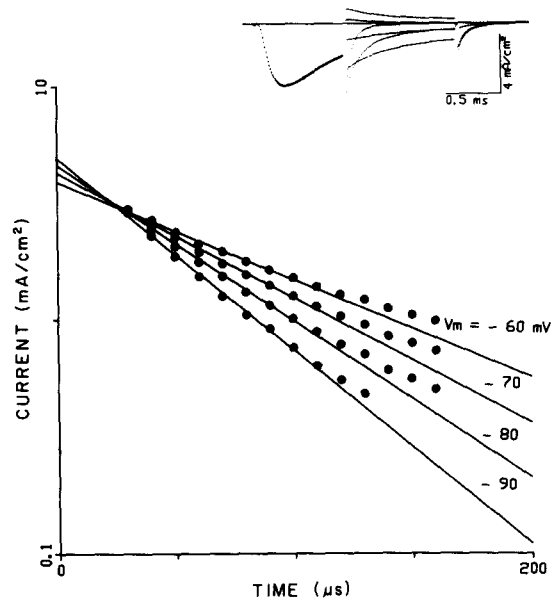
FIGURE 1. Sodium channel tail currents. The inset shows some TTX-corrected currents elicited with a conditioning membrane potential to +10 mV, lasting 0.8 ms and preceded by a hyperpolarizing pulse to −100 mV for 50 ms. The filled circles are tail current values for membrane potentials to −60, −70, −80, and −90 mV for a set of records similar to those shown on the inset but without the preconditioning hyperpolarizing pulse.

RESULTS

Block by External H^+ Is Modulated by Internal Permeant Cations

Fig. 3 shows peak sodium current-voltage relations in normal- and low-pH ASW for an axon perfused with 25 Na SIS and 125 Na SIS. Low external pH reduces sodium channel current and shifts the current-voltage curve in the depolarizing direction. The reduction in current can be seen to decrease as the membrane potential is made more positive. Also, the block is greater in 25 Na SIS than in 125 Na SIS, which can be seen more readily in Fig. 4, where the ratio of current in low pH to the average of control and recovery currents in normal pH is plotted.

Since the ordinate is the ratio of current remaining in low-pH ASW to that in normal-pH ASW, a value of unity in this plot represents no block. It is clear from Fig. 4 that there is less block as the membrane potential is made more positive. Also there is less block with 125 Na SIS as the perfusate than with 25 Na SIS. That is, raising the concentration of internal permeant ions reduces the ability of external hydrogen ions to block sodium channels.

Figs. 3 and 4 show another feature of the hydrogen ion effect: recovery currents at large positive potentials are sometimes larger than control. This effect occurs because low pH shifts the long-term inactivation curve in the depolarizing direction (Neumcke et al., 1976). Consequently, any inactivation present at normal pH can be removed at low pH. Since this is a very slow
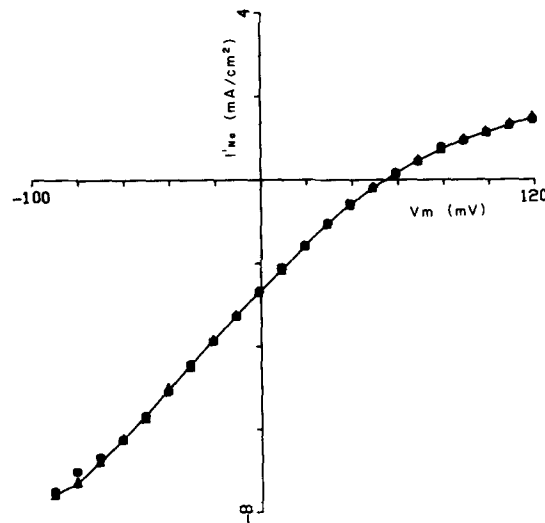

FIGURE 2. Sodium channel instantaneous current-voltage relation. Axon SQDJF bathed in 0-Mg ASW and perfused with 25 Na SIS. Instantaneous currents are plotted as a function of test potential both with (●) and without (▲) the hyperpolarizing prepulse to −30 mV (scaled by 1.68).

process (Adelman and Palti, 1969; Rudy, 1978), the observed results can occur if recovery measurements are made before the inactivation is restored to its resting value. This effect has been described previously for myelinated nerve (Woodhull, 1973; Neumcke et al., 1976). Another consequence of the action of H⁺ on slow inactivation is that the magnitude of block by low pH may be underestimated. The use of a more negative holding potential minimizes the effects of low pH on this slow inactivation, as seen in Fig. 5.

Fig. 5A illustrates that with a holding potential of −82 mV, low pH produces a much larger current reduction than in the axon of Fig. 4, for which the holding potential was −71 mV. The reduction of block by increased internal permeant ion concentration is still present. Fig. 5B shows a similar experiment but with different internal solutions: K SIS and 50 Na SIS. It

appears that 350 mM K is able to remove some of the hydrogen ion block present with 50 mM Na.

The current ratios in Figs. 4 and 5 were obtained with peak sodium channel currents. Over the voltage range from −40 to near 0 mV, these currents involve both the gating and the ionic permeation processes. Since
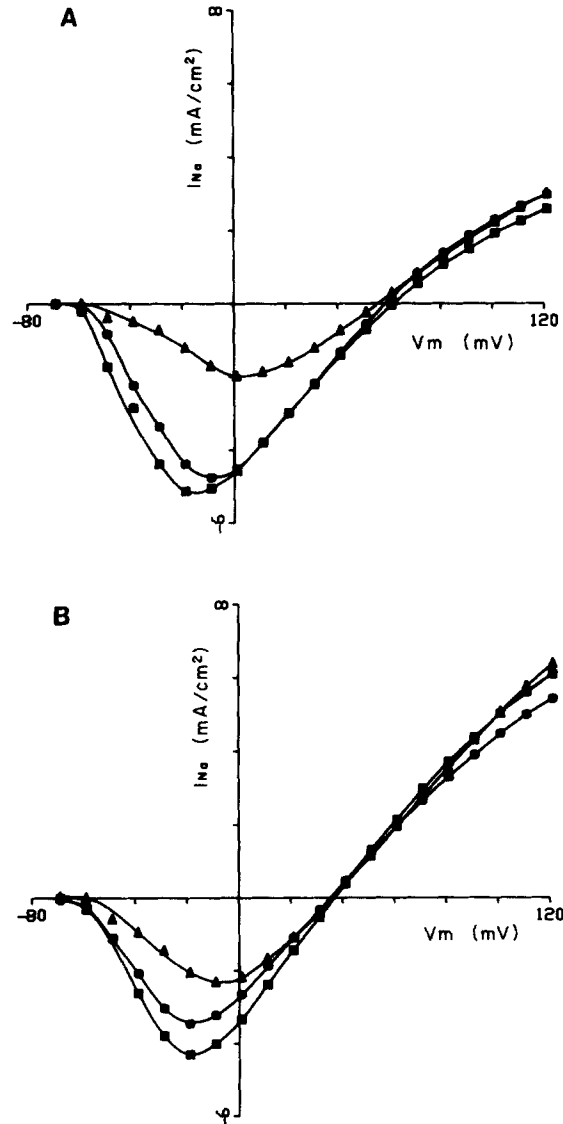
FIGURE 3. Sodium channel peak current-voltage relations for axon SQDKC in 0-Mg ASW. (A) Peak current-voltage relations shown with 25 Na SIS internally and external pH values of 7.5 (■, control; ●, recovery) and 4.8 (▲). (B) Peak current-voltage relations for the same axon and conditions of A but perfused with 125 Na SIS.

low pH is known to shift the sodium channel gating parameters toward more depolarizing potentials, peak currents include this shifting effect.

The ability of low pH to shift the voltage dependence of channel opening is illustrated in Fig. 6, where a measure of sodium channel activation (given by the normalized ratio of peak to instantaneous current) is plotted. The normal-pH data have been scaled to be unity at large potentials. The shifting effect of low pH is clearly seen at potentials between −30 and −60 mV, similar to results obtained by Carbone et al. (1978). This figure also shows that at normal pH the activation curve is the same in 25 and 125 Na SIS.

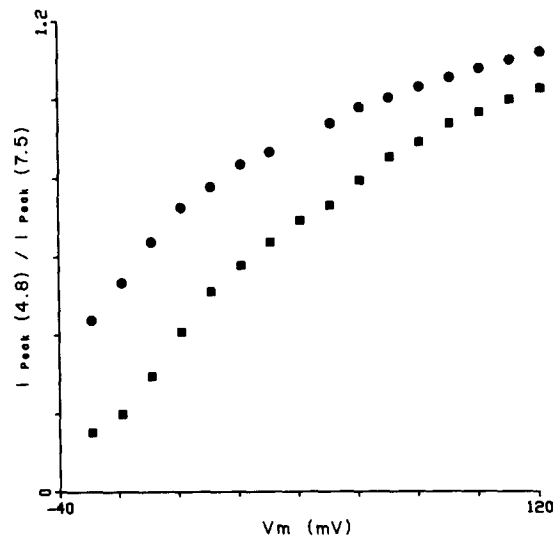To determine the voltage dependence of the hydrogen ion block inde-

FIGURE 4. Ratio of peak currents in low- and normal-pH 0-Mg ASW. The holding potential was −71 mV. The control and recovery (pH 7.5) current values from Fig. 3 were averaged before the ratio was calculated. Filled circles are with 125 Na SIS; the filled squares are for 25 Na SIS. Before the calculations were performed, the currents for pH 4.8 and pH 7.5 (recovery) were shifted by 4.4 and 1.9 mV, respectively, for 25 Na SIS and by 2.0 and 1.4 mV for 125 Na SIS. Axon SQDKC.

pendent of the effects on the gating process, we measured instantaneous currents using an activating pulse usually near +10 mV and occasionally at 0 mV. Not only is activation near maximum in this potential range (see Fig. 6), but the H⁺ block is relatively voltage independent near 0 mV (see Figs. 8, 9, and 10). Instantaneous current-voltage relations are shown in Fig. 7 for 25 and 125 Na SIS internal solutions.

It appears from this figure (and Fig. 3) that there is little or no change in the sodium channel current reversal potential, V_{rev}, when the external pH is lowered from 7.5 to 4.8. This was a consistent finding for all the internal solutions used, as the measured V_{rev} values in Table II demonstrate. The changes in reversal potential (ΔV_{rev}) in low-pH solutions are quite small and

vary in no consistent direction. Nevertheless, for voltages near the reversal potential where the currents are rather small, even such slight differences in V_{rev} can distort the computed ratio of current in low and normal pH. To avoid this distortion, all the instantaneous current-voltage relations from a
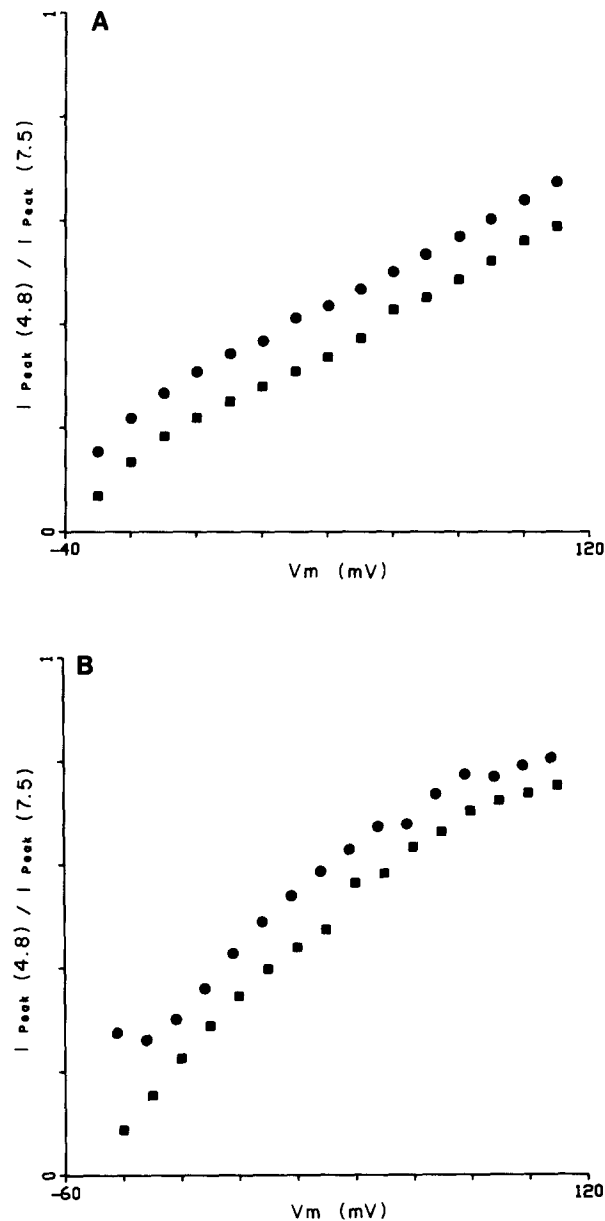

FIGURE 5.   Current ratios with negative holding potentials. (A) Axon SQDJN perfused with 125 Na SIS (●) and 25 Na SIS (■). A holding potential of −82 mV was used. (B) Axon SQDJK perfused with K SIS (●) and 50 Na SIS (■). The holding potential was −80 mV.

particular axon were shifted to match the value in the control solution. This was accomplished by fitting a third-order polynomial to two points above and two below the zero-current potential. The fitted curves were shifted until the zero-current potentials coincided. The average amount of this shift was 0.58 (SD = 2.3, n = 10), 0.04 ± 1.7 (9), −0.84 ± 3.4 (12), −0.4 ± 0.4 (4), and 0.05 ± 3.1 (9) mV for 25 Na, 125 Na, 50 Na, 200 Na, and K SIS solutions, respectively. Of the total of 44 values, only 3 were larger than 5 mV and these corresponded almost exactly to the amount of electrode drift determined at the end of the experiment. Although the amount of this correction was small, it provided substantially smoother current ratios at potentials near the reversal potential. After the current-voltage relations
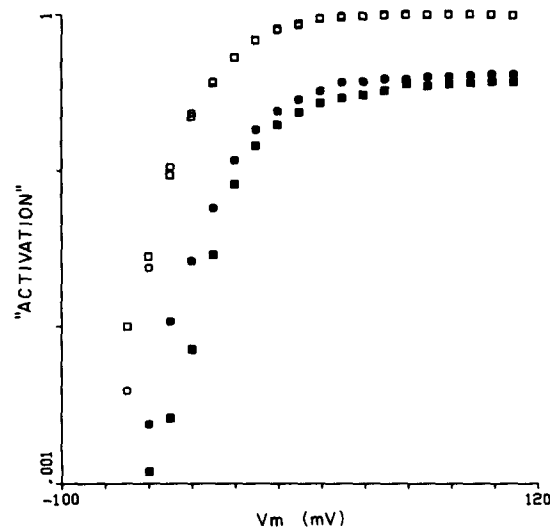

FIGURE 6.   Activation-voltage relation for axon SQDJN. The ordinate represents the peak sodium channel current divided by the instantaneous current at the potentials given by the abscissa. The pH 7.5 values have been normalized to unity at +90 mV. The squares and circles are for the 25 Na SIS and 125 Na SIS solutions, respectively. Open symbols represent pH 7.5 and filled symbols are for pH 4.8.

were shifted, a cubic spline function was used to interpolate between data points.

External H^+ Block Is a Nonmonotonic Function of Membrane Potential

Fig. 8 shows the ratio of instantaneous current values from the axon of Fig. 7 after corrections for the small differences in reversal potential described above. The ratios have been normalized so that the values near 0 mV correspond to the ratios of peak currents at 0 mV. There is clearly less block in the higher sodium solution. As expected from Figs. 4 and 5, the block is reduced at the depolarized end of the voltage range and is also relieved as the membrane potential is made more negative than zero. Similar results are illustrated with 50 and 200 Na SIS in Fig. 9.

In this figure the reduction of block by high internal sodium is seen. There is also the suggestion of a relief of block at negative potentials for the 50 Na SIS solution. But this point is much clearer in Fig. 10, where data from 10
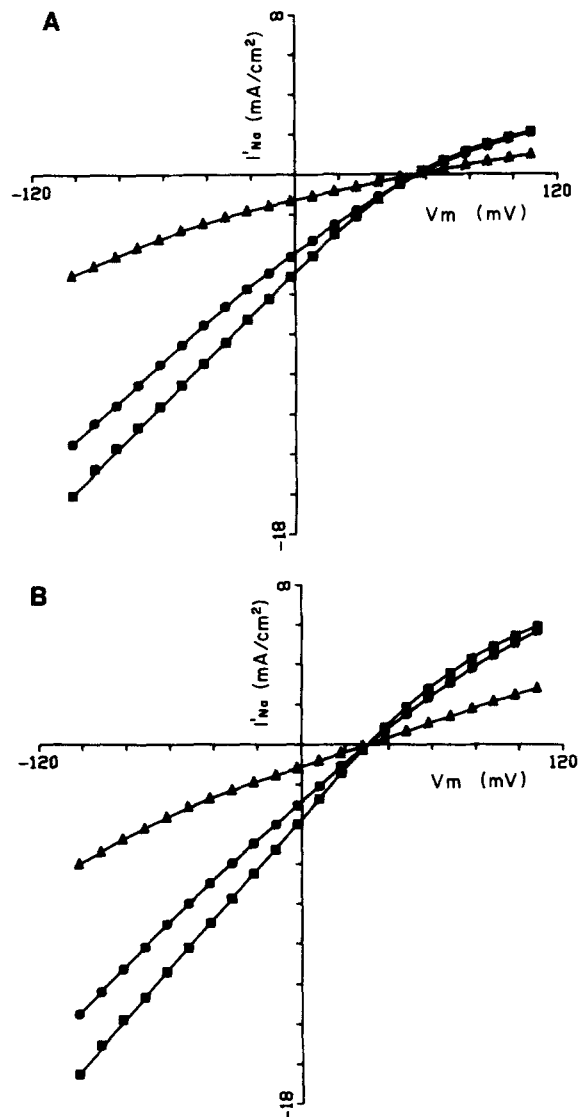

FIGURE 7.   Instantaneous sodium channel current-voltage relations for axon SQDJN perfused with 25 and 125 Na SIS. (A) A 200-ms preconditioning pulse to −102 mV was followed by a pulse to +40 mV for 0.6 ms at pH 7.5 (■, control; ●, recovery) and for 1.2 ms at pH 4.8 (▲). The membrane potential was then stepped to the values shown on the abscissa. The instantaneous currents were obtained as described in Methods. The internal solution was 25 Na SIS. (B) Same as A but the axon was perfused with 125 Na SIS. The holding potential was −82 mV.

TABLE II

Comparison of Reversal Potentials at Normal and Low External pH

Solution	V_{rev}		ΔV_{rev}
	Normal pH	Low pH	
	mV	mV	mV
50 Na SIS	52.5 ± 2.4 (18)	52.0 ± 3.7 (8)	−0.2
200 Na SIS	19.0 ± 0.17 (3)	19.5 ± 0.4 (3)	+0.5
25 Na SIS	55.4 ± 2.0 (5)	53.7 ± 2.5 (5)	−1.7
125 Na SIS	33.8 ± 4.1 (5)	32.9 ± 3.2 (5)	−0.9
K SIS	66.8 ± 4.0 (6)	67.3 ± 3.5 (6)	+0.5

axons perfused with 50 Na SIS are displayed. The 0-mV values of the ratios in Fig. 10 have all been scaled to match that of axon SQDJK. It can be seen that almost all the axons show a clear reduction in block at negative as well as positive potentials. The solid line represents the prediction of a three-barrier, two-site model for Na⁺ and H⁺ ion permeation, which is described in the Discussion.

Fig. 11 illustrates that the nonmonotonic, voltage-dependent block produced by external hydrogen ions is not induced by the internal perfusion technique. This figure shows the ratio of instantaneous currents in normal and low external pH for an intact (nonperfused) axon. As with the perfused axons, the block is largest near 0 mV and decreases with voltage in both directions, but more steeply in the depolarizing direction.
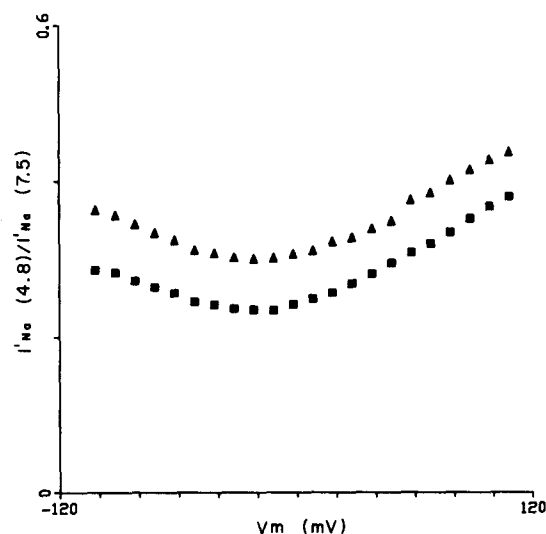

FIGURE 8. Ratio of instantaneous sodium channel currents in pH 4.8 and pH 7.5 0-Mg ASW. The control and recovery currents from Fig. 7 have been averaged and divided into the currents for pH 4.8. The ordinate values have been normalized so that the ratio of these currents is equal to the ratio of the peak currents at 0 mV for both 125 Na SIS (▲) and 25 Na SIS (■). The holding potential was −82 mV. Axon SQDJN.

DISCUSSION

Comparison with Previous Results

Several authors have reported the reduction of sodium channel currents in nerve by low external pH (Hille, 1968; Drouin and The, 1969; Woodhull, 1973; Shrager, 1974; Schauf and Davis, 1976). This current reduction has usually been interpreted as a block of the open pore by hydrogen ions. However, it is also possible to explain the reduction of sodium channel current produced by hydrogen ions as resulting from an interaction of hydrogen ions with the ionic channel gates rather than with the pore structure. Such a mechanism seems unlikely because hydrogen ions do not block sodium channel gating currents, but in fact actually enhance them (Neumcke
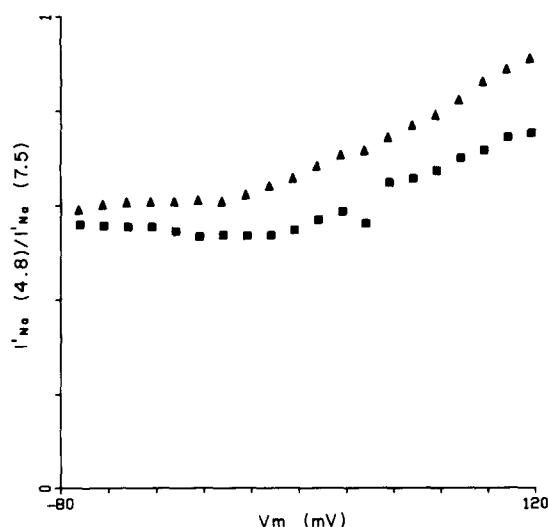

FIGURE 9. Ratio of instantaneous sodium channel currents in pH 4.8 and pH 7.5 0-Mg ASW. Similar to the data of Fig. 8, but this axon (SQDKG) was perfused with 200 Na SIS (▲) and 50 Na SIS (■). The holding potential was −72 mV.

et al., 1980). Similarly, it is difficult to reconcile such a mechanism with the reduction of single-channel currents (obtained with noise analysis) by low pH (Sigworth, 1980) and with the modulation of external hydrogen ion block by internal permeant ions seen here.

Previous measurements on other nerve preparations have yielded apparent pK_a values (near 0 mV) for the binding of hydrogen ions to the sodium pore of 5.2 (Hille, 1968) and 5.4 (Woodhull, 1973) for myelinated nerve and 4.8 for *Myxicola* giant axons (Schauf and Davis, 1976). Wanke et al. (1980) have reported a value of 4.6 for squid axons. We find apparent pK_a values of 4.95 and 4.88 with 50 Na and 200 Na SIS, respectively. The lower value of 4.6 obtained by Wanke et al. (1980) may reflect changes in long-term inactivation produced by low pH (as described above) or may result from the different internal and external solutions used in their experiments.

We find, in agreement with many previous observations, that the hydrogen ion block is reduced as the membrane is made more positive than zero. This effect has been explained by considering the binding site to be within the membrane electric field. Positive potentials would therefore decrease the probability of occupancy of such a site. However, Drouin and Neumcke (1974) have argued that an apparent voltage dependence can occur if there is an external surface charge that produces a local accumulation of permeant ions. The titration of this charge will reduce inward current with less effect on outward current. Such a surface charge would also produce a significant difference between the intrinsic and the apparent pK_a values.
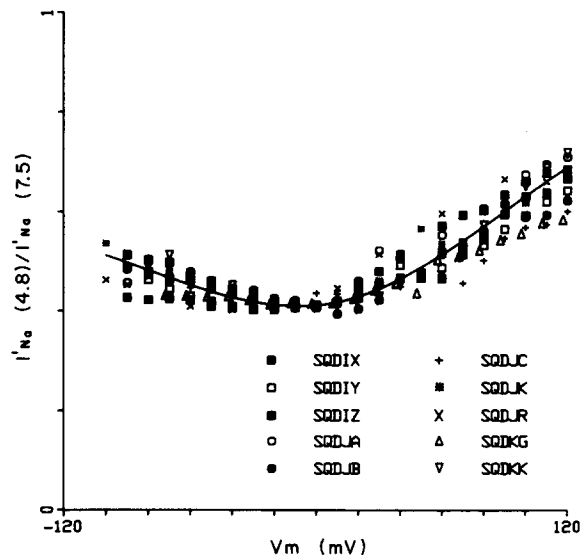
FIGURE 10.   Ratio of instantaneous sodium channel currents in pH 4.8 and pH 7.5 0-Mg ASW. Data from 10 axons perfused with 50 Na SIS are shown. Each axon is represented by a different symbol. The current ratios have all been normalized to the ratio of peak sodium currents at 0 mV of axon SQDJK. The solid line is the prediction of the simple three-barrier, two-site permeation model described in the Discussion.

Our observations demonstrate that such a mechanism would provide an incomplete description of hydrogen ion block. The relief of block at negative potentials cannot be accounted for by a simple surface-charge model. It is also difficult to reconcile the modulation of block by internal permeant ions with such a model.

One way of explaining the relief of hydrogen ion block at both positive and negative potentials is to assume a binding site within the membrane electric field and also to allow hydrogen ions to pass through the sodium channels (Woodhull, 1973). Recently, Mozhayeva et al. (1982) have used such a model to account for the nonmonotonic, voltage-dependent hydrogen ion block of sodium channels in myelinated nerve. In addition, they assumed

the existence of a second hydrogen ion binding site at the external surface of the pore.

There is clear evidence for several hydrogen ion binding sites. Spalding (1980) and Sigworth and Spalding (1980) have shown that a carboxyl-modifying reagent, trimethyloxonium ion, inhibits TTX block of sodium channels but preserves hydrogen ion block. They suggest that the carboxyl group important for TTX binding is near enough to the pore mouth to influence the pK_a of the primary hydrogen ions binding site discussed in our paper. There are also other observations that suggest that there is not much surface charge near the pore mouth (Begenisich, 1975; Henderson et al., 1973).

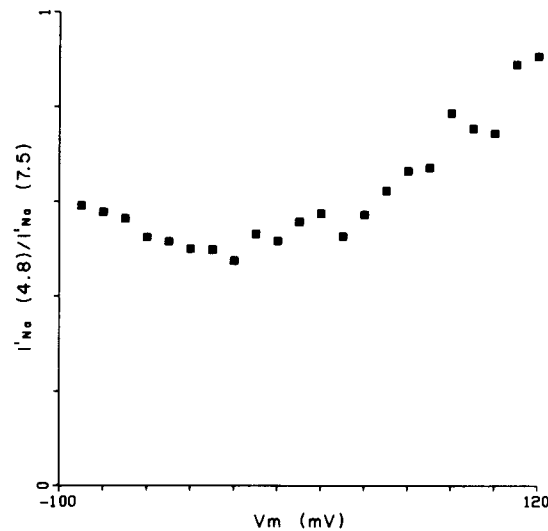In the absence of a direct demonstration of the existence or absence of

FIGURE 11.   Ratio of instantaneous currents for pH 4.8 and pH 7.5 0-Mg ASW. Similar to Figs. 8, 9, and 10 but for a nonperfused axon (SQDIT). The holding potential was −71 mV.

such local surface charges, we have chosen to describe our results with a model that ignores them. The fact that we are able to account for our observations without considering surface charges is satisfying, but certainly is not a definitive argument against the presence of fixed surface charges near sodium pores. Clearly, more experimental work on this subject is necessary.

Recently, Campbell (1982) studied hydrogen ion block of sodium channels in frog skeletal muscle. Several differences in experimental and analytical techniques make a detailed comparison with our results difficult. Campbell (1982) used isochronal rather than instantaneous currents to assay the block. These currents were converted to permeabilities via the constant field equation. The low-pH permeability-voltage curve was shifted along the voltage axis. He believes from his experiments that block by hydrogen ions is not

described by the Woodhull model but rather is voltage independent. With our different technique and preparation, we agree that block cannot be described by a simple Boltzmann relation, but we do not confirm that it is voltage independent.

A Mathematical Model for Hydrogen Ion Block

A three-barrier, two-site model for ion permeation through sodium pores has been described (Begenisich and Cahalan, 1980a, b). This same model can account for more recent data on unidirectional ionic fluxes through sodium channels of squid giant axons (Begenisich and Busath, 1981; Busath and Begenisich, 1982). We have therefore investigated the ability of this model to describe the results of this study.
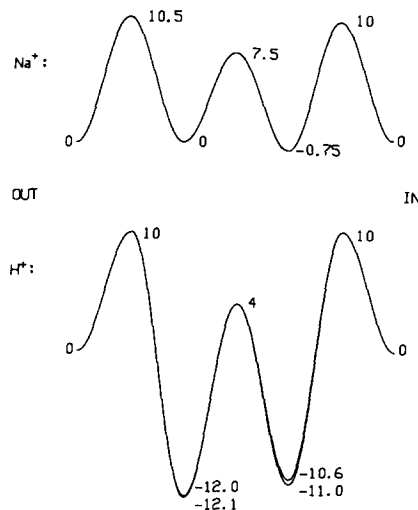
FIGURE 12.   Sodium and hydrogen ion barrier profiles for the three-barrier, two-site models described in the Discussion. The barrier heights and well depths are given in RT units. The barriers are symmetrically shaped and the wells are equally spaced along the membrane electric field.

The three-barrier, two-site model views the ion permeation pathway as a sequence of energy barriers and wells. The permeating ions "jump" (according to a Poisson process) from well to well with a rate that decreases exponentially with the height of the intervening energy barrier (Eyring et al., 1949). The energy barriers and wells that a sodium ion encounters as it traverses the pore are shown in the upper part of Fig. 12. (The details of how these parameters were obtained are described in Begenisich and Cahalan [1980a, b].) This model allows for the simultaneous occupancy of the pore by two ions.

We do not yet have sufficient data to determine with absolute certainty the appropriate barriers and wells for hydrogen ions; however, Fig. 12 illustrates two possible sets of parameters. For simplicity, the barrier heights

for hydrogen ions were assumed to be symmetrical, and the wells equally spaced. The values shown were chosen to fit the data of Fig. 10. The less negative values of the well depths ($-12.0RT$ and $-10.6RT$) were used to compute the solid line in Fig. 10: clearly a reasonable representation of the data. The other values of the hydrogen ion wells are used in a modified version of the model described later.

Our experiments show that raising the concentration of internal permeant ions reduces the blocking action of external hydrogen ions: 200 Na SIS increases the relative current by a factor of ~ 1.1 at 0 mV and by ~ 1.15 at +100 mV. This simple three-barrier, two-site model with the energy profiles of Fig. 12 (H^+ ion well depths of $-12.0RT$ and $-10.6RT$) predicts lower values of just slightly larger than unity and 1.06 at 0 and 100 mV, respectively. Although there is a qualitative agreement between the model and the data, it fails to predict the proper quantitative behavior in 200 Na SIS.

The model explains the decrease in block produced by permeant ions by a competition between these ions and hydrogen ions for the sites within the pore. The decrease in block at positive potentials occurs because depolarized potentials prevent the binding of hydrogen ions within the pore. The relief of block at negative potentials results from the hydrogen ions being driven through the pore.

According to this model, hydrogen ions are two to three times more permeant than sodium ions. Mozhayeva et al. (1982) estimate from changes of V_{rev} in low-pH solutions a hydrogen-to-sodium permeability ratio for sodium channels in myelinated nerve of 274. Although there is certainly a quantitative difference between these estimates, we are in agreement that hydrogen ions may be relatively permeant through sodium channels.

In trying to fit our data on the effects of external hydrogen ions, we considered the results of Wanke et al. (1980) on internal hydrogen ion block of sodium channel current. These authors did not measure instantaneous current-voltage relations, and changes in slow inactivation probably affected their results to some extent. Nevertheless, they found that more positive membrane potentials decreased the block produced by low internal pH. In analogy with our explanation for the reduction of external H^+ block at

FIGURE 13. (opposite) Theoretical ratio of currents. The sodium barriers shown at the top of Fig. 12 were used for all computations. (A) Ratio of currents for external pH values of 4.8 and 7.5. The calculations resulting in curve 1 used the hydrogen ion barriers shown in the bottom of Fig. 11 and well depths of -12.0 and -10.6. Calculations using hydrogen ion well depths of -12.1 and -11.0 and ionic repulsion are shown as curve 2. Curve 3 illustrates the reduction of block expected for a 200-Na solution using the same parameters as for curve 2. The external sodium concentration used for the calculations was 440 mM. (B) Ratio of currents for internal pH values of 5 and 7.5. Curves 1 and 2 are the predictions of the three-barrier, two-site models with the same parameter as curves 1 and 2 in A. The external and internal sodium concentration used in the calculation were 110 and 200 mM, respectively, simulating the conditions of Wanke et al. (1980).

negative membrane potentials, it seems reasonable to ascribe this effect to the clearing of the pore by hydrogen ions permeating through it.

Using the sodium barriers described above, we could not find one set of hydrogen ion barriers that accurately accounted for the voltage dependence of both internal and external hydrogen ion block. Parameter changes that improved the fit for one made it worse for the other. The hydrogen ion barriers and wells used for Fig. 10 are the best that can be done with this simple model. It predicts the results shown in Fig. 13*B* (curve 1) for internal
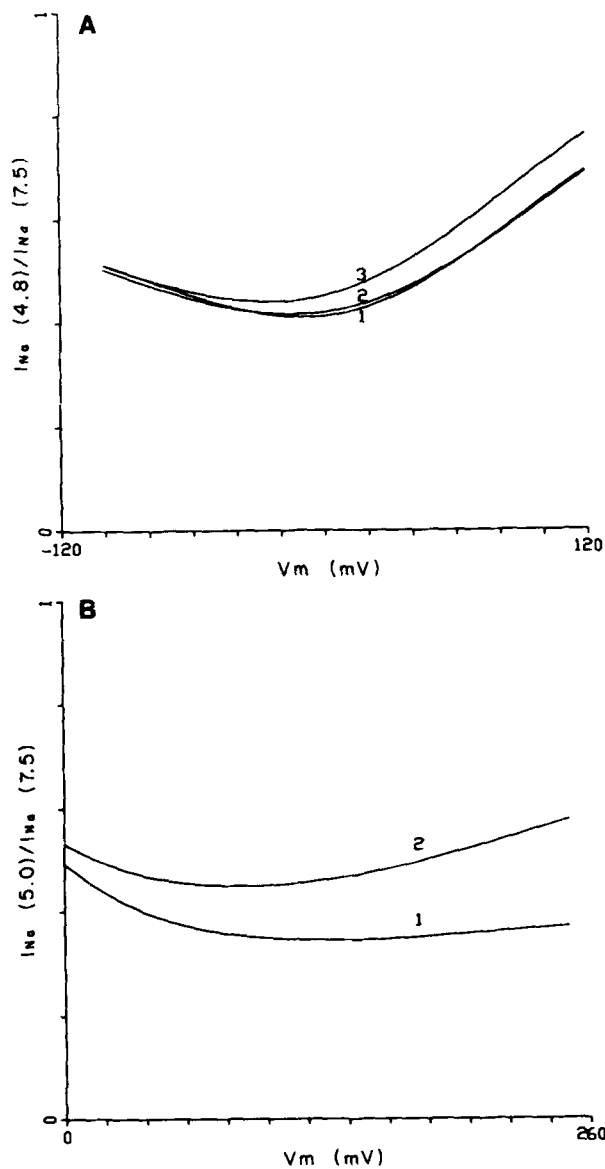
hydrogen ion block. The solutions used for this simulation approximate those used by Wanke et al. (1980). The block is larger than that reported, and there is little relief of block at large positive potentials.

A way to improve the model to better describe both the reduction of block by high internal sodium and the internal pH results is to include ionic repulsion between ions within the pore. The model for hydrogen ion block of sodium channels in myelinated nerve recently reported by Mozaheyeva et al. (1982) also includes ionic repulsion with the pore.

The concept of ionic repulsion in pores has been discussed by Hille and Schwarz (1978) and Begenisich and Cahalan (1980a). Like Hille and Schwarz (1978), we add repulsion in the model by including a factor F describing the effect of an ion occupying one site on the rate of jumping of another ion into or out of the second site. Accordingly, we increase the rate of leaving the second site by F and decrease the rate of entering by $1/F$. Hille and Schwarz suggest that, depending on the pore structure, F^2 may take on extreme values between 2 and 500.

Computations for the three-barrier, two-site model with a value of F equal to 4 are plotted in Fig. 13, A and B (curves labeled 2). The hydrogen ion wells in this case are -12.1 and -11.0 shown in the lower part of Fig. 12. For comparison, curves 1 in Fig. 13, A and B, are obtained from the model without ion repulsion. Fig. 13A demonstrates that there is little difference between the two models for 50 mM internal sodium. However, raising internal sodium to 200 mM reduces the expected block for the model with ionic repulsion by 1.08 at 0 mV and by ~ 1.12 at $+100$ mV, close to the experimental values described above. Fig. 13B shows that the presence of ionic repulsion reproduces better the block by internal hydrogen ions, especially the reduction of block at large positive potentials.

A Molecular Picture of the Sodium Pore

Hille (1975) has described a molecular interpretation of a four-barrier model for permeation through sodium channels in myelinated nerve. Since that report appeared, much new evidence has been obtained that helps to form a more complete molecular picture of the pore. Begenisich and Cahalan (1980a, b) showed that there was a binding site for Na^+ and other permeant cations near the axoplasmic end of the pore but within the membrane electric field. The presence of such a structure is supported by the finding of a H^+ binding site near the axoplasmic end of the sodium pore (Wanke et al., 1980). The present work and that of Wanke et al. (1980) demonstrate the existence of a hydrogen ion binding site within but near the external end of the pore.

These various results probably indicate that at least three acid groups constitute integral parts of the sodium pore. One is outside but near the external opening of the pore and is part of the receptor for TTX. The other two are within the pore but near the ends and bind permeant ions like sodium and blocking ions like hydrogen. The inner site provides a receptor for hydrogen ions and perhaps for impermeant blocking ions.

CONCLUSIONS

We find that the external hydrogen ion block of squid axon sodium channels is a nonmonotonic function of voltage. This block occurs within the sodium permeation pathway since internal permeant ions modify the block. The decrease of hydrogen ion block at positive potentials is probably a voltage-dependent exclusion of hydrogen ions from the blocking site. The decrease of block at negative potentials is consistent with hydrogen ions having a relatively high permeability through sodium channels. We have been able to account for these effects with a simple three-barrier, two-site model for ion permeation. If this model is modified to include ionic repulsion within the pore, it can also account for internal hydrogen ion block.

REFERENCES

Adelman, W. J., Jr., and Y. Palti. 1969. The effects of external potassium and long duration voltage conditioning on the amplitude of sodium currents in the giant axon of the squid *Loligo pealei. J. Gen. Physiol.* 54:589–606.

Begenisich, T. 1975. Magnitude and location of surface charges on *Myxicola* giant axons. *J. Gen. Physiol.* 66:47–65.

Begenisich, T., and D. Busath. 1981. Sodium flux ratio in voltage-clamped squid giant axons. *J. Gen. Physiol.* 77:489–502.

Begenisich, T., and M. D. Cahalan. 1980a. Sodium channel permeation in squid axons. I. Reversal potential experiments. *J. Physiol. (Lond.).* 307:217–242.

Begenisich, T., and M. D. Cahalan. 1980b. Sodium channel permeation in squid axons. II. Non-independence and current-voltage relations. *J. Physiol. (Lond.).* 307:243–257.

Begenisich, T., and M. Danko. 1982. Hydrogen ion block of sodium channels of squid giant axons. *Biophys. J.* 37:103a. (Abstr.)

Begenisich, T., and C. Lynch. 1974. Effects of internal divalent cations on voltage-clamped squid axons. *J. Gen Physiol.* 63:675–689.

Busath, D., and T. Begenisich. 1982. Unidirectional sodium and potassium fluxes through the sodium channel of squid giant axons. *Biophys. J.* 40:41–49.

Campbell, D. T. 1982. Do protons block Na⁺ channels by binding to a site outside the pore? *Nature (Lond.).* 298:165–167.

Campbell, D. T., and B. Hille. 1976. Kinetic and pharmacological properties of the sodium channel of frog skeletal muscle. *J. Gen. Physiol.* 67:309–323.

Carbone, E., R. Fioravanti, G. Prestipino, and E. Wanke. 1978. Action of extracellular pH on Na⁺ and K⁺ membrane currents in the giant axon of *Loligo vulgaris. J. Membr. Biol.* 43:295–315.

Drouin, H., and B. Neumcke. 1974. Specific and unspecific charges at the sodium channels of the nerve membrane. *Pflügers Arch. Eur. J. Physiol.* 351:207–229.

Drouin, H., and R. The. 1969. The effect of reducing extracellular pH on the membrane currents of the Ranvier node. *Pflügers Arch. Eur. J. Physiol.* 313:80–88.

Eyring, H., R. Lumry, and J. W. Woodbury. 1949. Some applications of modern rate theory to physiological systems. *Rec. Chem. Prog.* 100:100–114.

Henderson, R., J. M.-Ritchie, and G. R. Strichartz. 1973. The binding of labelled saxitoxin to the sodium channels in nerve membranes. *J. Physiol. (Lond.).* 235:783–804.

Hille, B. 1968. Charges and potentials at the nerve surface. Divalent ions and pH. *J. Gen. Physiol.* 51:221–236.

Hille, B. 1975. Ionic selectivity, saturation, and block in sodium channels. A four-barrier model. *J. Gen. Physiol.* 66:535–560.

Hille, B., and W. Schwarz. 1978. Potassium channels as multi-ion single-file pores. *J. Gen. Physiol.* 72:409–442.

Mozhayeva, G. N., A. P. Naumov, and Yu. A. Negulyaev. 1982. Interaction of H^+ ions with acid groups in normal sodium channels. *Gen. Physiol. Biophys.* 1:5–19.

Neumcke, B., J. M. Fox, H. Drouin, and W. Schwarz. 1976. Kinetics of the slow variation of peak sodium current in the membrane of myelinated nerve following change of holding potential or extracellular pH. *Biochim. Biophys. Acta.* 426:245–257.

Neumcke, B., W. Schwarz, and R. Stampfli. 1980. Increased charge displacement in the membrane of myelinated nerve at reduced extracellular pH. *Biophys. J.* 31:325–332.

Rudy, B. 1978. Slow inactivation of the sodium conductance in squid giant axons. Pronase resistance. *J. Physiol. (Lond.).* 283:1–21.

Schauf, C. L., and F. A. Davis. 1976. Sensitivity of the sodium and potassium channels of *Myxicola* giant axons to changes in external pH. *J. Gen. Physiol.* 67:185–195.

Shrager, P. 1974. Ionic conductance changes in voltage-clamped crayfish axons at low pH. *J. Gen. Physiol.* 64:666–690.

Sigworth, F. J. 1980. The conductance of sodium channels under conditions of reduced current at the node of Ranvier. *J. Physiol. (Lond.).* 307:131–142.

Sigworth, F. J., and B. C. Spalding. 1980. Chemical modification reduces the conductance of sodium channels in nerve. *Nature (Lond.).* 283:293–295.

Spalding, B. C. 1980. Properties of toxin resistant sodium channels produced by chemical modification in frog skeletal muscle. *J. Physiol. (Lond.).* 305:485–500.

Taylor, R. E., C. M. Armstrong, and F. Bezanilla. 1976. Block of sodium channels by external calcium ions. *Biophys. J.* 16:27a. (Abstr.)

Wanke, E., E. Carbone, and P. L. Testa. 1980. The sodium channel and intracellular H^+ blockage in squid axons. *Nature (Lond.).* 287:62–63.

Woodhull, A. M. 1973. Ionic blockage of sodium channels in nerve. *J. Gen. Physiol.* 61:687–708.